Joint Power Allocation and Constellation Rotation in Alamouti coded Interference Alignment in X-Channel with imperfect CSI

H. Khaleghi Bizaki[1*], E. Rahimi[2]

[1,2]Deparement of Electrical and Computer Engineering, Malek Ashtar University of Technology, Tehran, Iran.
Email: bizaki@yahoo.com, siperisck@yahoo.com.
[*]Corresponding Author

Received 15 September 2012, Revised 15 August 2013, Accepted 22 August 2013

Abstract

Interference Alignment (IA) with Alamouti coding is an innovative method to increase the multiplexing gain and the diversity gain, simultaneously, in wireless Multiple-Input Multiple-Output (MIMO) systems. The main limitation of this method is requiring Perfect Channel State Information (CSI) to perform the beamforming on transmitters and receivers signals. Contrary to the acceptable performance of Alamouti coding in perfect CSI conditions, its efficiency is severely reduced in imperfect CSI conditions. In order to overcome this shortcoming, this paper discusses about the effect of imperfect CSI on a two user MIMO X-channel which uses interference alignment together with Alamouti coding. Also, a closed form solution is extracted for the received signal in an imperfect CSI scenario. Our analysis shows that when the variance of the CSI error is increased, the Bit Error Rate (BER) of system increases linearly. Also, we propose a joint Power Allocation (PA) and constellation rotation algorithm to improve the performance of system in an imperfect CSI scenario. Computer simulations show a desirable improvement in BER by using PA, constellation rotation and joint of them.

Keywords

Interference alignment, Alamouti coding, Channel state information, Power Allocation, Constellation Rotation.

1. Introduction

Interference Alignment (IA) is one of the most interesting issues in recent researches because of significant improvement in data rate of interfering wireless networks. In IA method, transmit signal subspace is managed by beamforming in transmitter and receiver, so that each user receives it's desired signal in an independent subspace and interfering signals in a common subspace with a much lower dimension than the number of interfering signals. Hence, more dimensions of signal space assigned to the desired signal which in turn lead to more system multiplexing gain.

In the articles [1-4] some ideal conditions is considered for IA such as: access to global and perfect channel information in both transmitter (TX) and receiver (RX) sides, infinite signal stream length and infinite Signal to Noise Ratio (SNR) in which are practically impossible [5]. These limitations attracted researcher's attentions to solve them and some IA methods with finite signal stream length is proposed in [5,6]. Although, IA with partial CSI [7, 8] or imperfect CSI [9-11] is discussed and some solutions were proposed and even some considerable results were achieved in terms of Blind Interference Alignment (BIA) [12-14] in some special cases, however, a global closed form method to use IA with no CSI or imperfect CSI is still an open problem.

In [15] a performance analysis of interference alignment (IA) over MIMO interference channels has been done and a closed-form expression of outage probability, ergodic rate and SER are derived. In [16] imperfect CSI on the sum-rate performance of IA system, in multiple-input multiple-output (MIMO) cellular networks is analyzed. Based on the 3GPP spatial channel model (SCM), they obtained the relationships between the sum rate loss and all factors that cause the imperfect CSI. A combining scheme of interference alignment and Alamouti codes is proposed in [17] for the quasistatic MIMO $K\times 2$ X-channel. They proposed transmission and decoding schemes that exploits the zero-forcing and decoupling method of two Alamouti-codes. Performance analysis of Alamouti scheme with imperfect CSI for a multiple-input-single-output (MISO) communications system discussed in [18].

The use of IA to mitigate inter-cell interference of cellular networks under imperfect CSI conditions is studied in [19] based on stochastic geometry. In [20], interference cancellation (IC) scheme based on Alamouti code in the multiple access scenario is applied to the K-user, MIMO interference channel. In order to reduce the number of receive antennas, they proposed an IA-and Cancellation (IAC) scheme based on

Alamouti code. The authors in [21] designs a beamformer using interference alignment scheme with Alamouti codes ove M×2 X-channels in perfect CSI.

Unfortunately, in all mentioned papers [15-21], the authors do not proposed any solution to improve interference alignment of Alamouti codes in imperfect CSI.

Interference cancellation scheme without feedback is proposed in [22] for X-channels with four antennas at each user based on a Space-time code with Alamouti structure together with multi-user interference mitigation by the orthogonal property of the Alamouti code in perfect CSI. Also, an interference alignment scheme based on the errors-in-variables (EIV) mathematic model has been proposed in [23] to overcome the channel state information (CSI) estimation error for the MIMO interference channels. These authors proposed an iterative algorithm weighted total least squares (WTLS) method for transmit precoding (TPC) matrices calculation which severely sufferers from computational complexity due to needs about 100 iteration. In this research, as well as the mentioned works, interference alignment is studied in MIMO X-channel because of its generality in communications channels.

According to previous articles, in this paper, we investigate the effect of CSI imperfectness on Bit Error Rate (BER) of system and propose a closed form solution for received signal which is divided into four terms as: desired signal, interference signal error, desired signal error and noise to declare the performance degradation. Then, we propose Power Allocation (PA) and Constellation Rotation (CR) method to improve the system BER under imperfect CSI conditions. Finally, we combine these two methods as joint Power Allocation and Constellation Rotation (PA-CR) to achieve more performance improvement of system.

The rest of the paper is organized as follows: problem statement and basic information is declared in section 2. The effect of imperfect CSI on system is analyzed in section 3 and some computer simulations are prepared to show its performance degradation. In section 4 and 5 we propose Power Allocation (PA) method and Constellation Rotation (CR) method to improve the system performance and show their effects on BER performance. Computer simulations of the proposed method together with the analysis of the results are discussed in section 5. The joint power allocation and constellation rotation, as PA-CR method, is simulated at the end of section 5 to achieve better performance. Finally, we conclude our results in section 6.

Notation: We use lowercase alphabet for definition of scalar values, bold lowercase for vectors and uppercase for matrixes. Likewise, A^t, A^*, A^{H} and $\|A\|$ denote transpose, conjugate, hermitian and Frobenius norm of matrix A. Also, $E(.)$ denotes Expectation operation and $vec(\boldsymbol{x})$ is a vectorized form of vector $\boldsymbol{x}$.

2. Problem Statement

Consider an X-channel which has two double-antennas at transmitter and two double-antennas at receiver. The i^{th} transmitter sends independent messages to the j^{th} receiver in time slot (k) which is shown by s_{ij}^{k}. As it is shown in figure (1), the channel coefficients matrix is broken to H, A, G and B which are channel coefficient matrix from transmitter 1 to receiver 1, transmitter 1 to receiver 2, transmitter 2 to receiver 1 and transmitter 2 to receiver 2, respectively which their components assumed to be independent and identical distribution (i.i.d.) of Complex Normal distribution as $\mathcal{CN}(0,1)$. Also, we assume that the channel coefficients are constant during the transmission. Each transmitter knows only it's own channel information to both receivers and encodes messages in Alamouti structure and sends block matrix X_i in two time slots. Thus, each user receives signal in the following form:

$$Y_1 = X_1 H + X_2 G + W_1 \tag{1}$$

$$Y_2 = X_1 A + X_2 B + W_2 \tag{2}$$

where X_1 and X_2 are defined in (3), (4) and W_j for $j = 1,2$ is unit variance zero mean additive white Gaussian noise (AWGN) in the j^{th} double-antennas receiver.

A method is proposed in [8] which combine IA and Alamouti coding in X-channel to attain maximum achievable multiplexing gain of $\frac{8}{3}$ [4], and maximum diversity gain, which is 2 for Alamouti coding, without loss of multiplexing gain. In this section, we briefly explain this method and then develop their analysis in the next section.

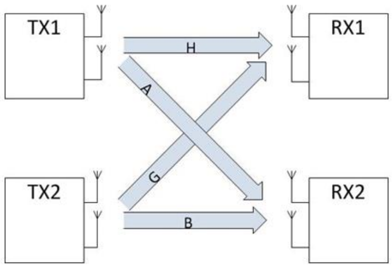

Fig. 1. System model of X- Channel

Each transmitter sends two symbols to each receiver in a three timeslot which is formed as follows[8]:

$$X_1 = \sqrt{\frac{3P}{2}}\left(\begin{bmatrix} s_{11}^1 & s_{11}^2 \\ -s_{11}^{2*} & s_{11}^{1*} \\ 0 & 0 \end{bmatrix} V_{11} + \begin{bmatrix} 0 & 0 \\ -s_{12}^{2*} & s_{12}^{1} \\ s_{12}^{1} & s_{12}^{2} \end{bmatrix} V_{12}\right) \tag{3}$$

$$X_2 = \sqrt{\frac{3P}{2}}\left(\begin{bmatrix} s_{21}^1 & s_{21}^2 \\ -s_{21}^{2*} & s_{21}^{1*} \\ 0 & 0 \end{bmatrix} V_{11} + \begin{bmatrix} 0 & 0 \\ -s_{22}^{2*} & s_{22}^{1} \\ s_{22}^{1} & s_{22}^{2} \end{bmatrix} V_{12}\right) \tag{4}$$

where V_{ij} is 2×2 beamforming matrix from transmitter i to receiver j, and P is the transmit power. These matrices are formed to align 2nd receiver's desired signals in first receiver and occupy one dimension of signal space. Similarly, first receiver's desired signals is aligned in one dimension in second receiver. These beamforming matrices are generated from CSI as following [8]:

$$V_{11} = \frac{A^{-1}}{\|A^{-1}\|} \qquad , \qquad V_{12} = \frac{H^{-1}}{\|H^{-1}\|}$$

$$V_{21} = \frac{B^{-1}}{\|B^{-1}\|} \quad , \quad V_{22} = \frac{G^{-1}}{\|G^{-1}\|} \tag{5}$$

The above coefficient terms satisfy the unity condition as $(V_{ij}V_{ij}^{*}) = 1$. Thus, the SNR remains constant. Setting equations (3), (4) and (5) in (1) and (2) yields [8]:

$$Y_1 = \sqrt{\frac{3P}{2}}\begin{bmatrix} s_{11}^1 & s_{11}^2 \\ -s_{11}^{2*} & s_{11}^{1*} \\ 0 & 0 \end{bmatrix} V_{11}H + \sqrt{\frac{3P}{2}}\begin{bmatrix} s_{21}^1 & s_{21}^2 \\ -s_{21}^{2*} & s_{21}^{1*} \\ 0 & 0 \end{bmatrix} V_{21}G + \sqrt{\frac{3P}{2}}\begin{bmatrix} 0 & 0 \\ -as_{12}^{2*}-bs_{22}^{2*} & as_{12}^{1*}+bs_{22}^{1*} \\ as_{12}^{1}+bs_{22}^{1} & as_{12}^{2}+bs_{22}^{2} \end{bmatrix} + W_1$$

$$Y_2 = \sqrt{\frac{3P}{2}}\begin{bmatrix} 0 & 0 \\ -s_{12}^{2*} & s_{12}^{1*} \\ s_{12}^1 & s_{12}^2 \end{bmatrix} V_{12}A + \sqrt{\frac{3P}{2}}\begin{bmatrix} 0 & 0 \\ -s_{22}^{2*} & s_{22}^{1*} \\ s_{22}^1 & s_{22}^2 \end{bmatrix} V_{22}B + \sqrt{\frac{3P}{2}}\begin{bmatrix} cs_{11}^1+ds_{21}^1 & cs_{11}^2+ds_{21}^2 \\ -cs_{11}^{2*}-ds_{21}^{2*} & cs_{11}^{1*}+ds_{21}^{1*} \\ 0 & 0 \end{bmatrix} + W_2 \tag{6}$$

where $=\frac{\sqrt{2}}{\|H^{-1}\|}$, $b = \frac{\sqrt{2}}{\|G^{-1}\|}$, $c = \frac{\sqrt{2}}{\|A^{-1}\|}$, $d = \frac{\sqrt{2}}{\|B^{-1}\|}$ and W_i are AWGN with zero mean and unit variance (i.e. $\mathcal{CN}(0,1)$). It can be observed that s_{12}^k and s_{22}^k in first and consequently s_{21}^k and s_{11}^k in second receivers are aligned. So, each receiver can decode its desired signals in independent dimensions and interference is collected in a common dimension. In this method, each transmitter must have access to its own channel information perfectly to beamform transmitted signals and there is no need to global CSI in all nodes. However, CSI perfectness is still an important limitation in this method. In the next section, we analyze the effect of this limitation and try to find a closed form solution for receiver error.

To simplify notation, assume $\tilde{H} = V_{11}H$, $\tilde{G} = V_{21}G$, $\tilde{A} = V_{12}A$ and $\tilde{B} = V_{22}B$.

3. Performance Analysis with imperfect CSI

Assume that the channel estimator is imperfect and the real (or perfect) channel coefficients are modeled as following normalized form [15]:

$$\begin{aligned} \bar{H} &= \left(\sqrt{1-\rho^2}\right)H + \rho(\Delta H) \\ \bar{A} &= \left(\sqrt{1-\rho^2}\right)A + \rho(\Delta A) \\ \bar{G} &= \left(\sqrt{1-\rho^2}\right)G + \rho(\Delta G) \\ \bar{B} &= \left(\sqrt{1-\rho^2}\right)B + \rho(\Delta B) \end{aligned} \tag{7}$$

where ρ^2 is the estimator's error variance. The matrices ΔH, ΔA, ΔG and ΔB are estimation error of H,A,G and B ,respectively, which have a distribution as $\mathcal{CN}(0,1)$. To reduce complexity of notation we consider the estimated channel coefficients as H,A,G and B and perfect channel coefficient as $\bar{H}$,$\bar{A}$,$\bar{G}$ and $\bar{B}$. The imperfect channel estimation causes beamforming error at the transmitter and Alamouti decoding error at the receiver side as we discuss in the sequel.

3.1. The effect of channel error on Transmitted signal

With the assumption of channel estimation error similar to (7), the imperfect CSI in beamforming equation (6) can be expressed as:

$$\begin{aligned} Y'_1 = \sqrt{\frac{3P}{2}}\Bigg(&\begin{bmatrix} s_{11}^1 & s_{11}^2 \\ -s_{11}^{2*} & s_{11}^{1*} \\ 0 & 0 \end{bmatrix}\frac{A^{-1}}{\|A^{-1}\|}.\left(\left(\sqrt{1-\rho^2}\right)H + \rho\Delta H\right) + \begin{bmatrix} s_{21}^1 & s_{21}^2 \\ -s_{21}^{2*} & s_{21}^{1*} \\ 0 & 0 \end{bmatrix}\frac{B^{-1}}{\|B^{-1}\|}.\left(\left(\sqrt{1-\rho^2}\right)G + \rho\Delta G\right) \\ &+ \begin{bmatrix} 0 & 0 \\ -s_{12}^{2*} & s_{12}^{1*} \\ s_{12}^1 & s_{12}^2 \end{bmatrix}\frac{H^{-1}}{\|H^{-1}\|}.\left(\left(\sqrt{1-\rho^2}\right)H + \rho\Delta H\right) + \begin{bmatrix} 0 & 0 \\ -s_{22}^{2*} & s_{22}^{1*} \\ s_{22}^1 & s_{22}^2 \end{bmatrix}\frac{G^{-1}}{\|G^{-1}\|}.\left(\left(\sqrt{1-\rho^2}\right)G + \rho\Delta G\right)\Bigg) + W'_1 \end{aligned} \tag{8}$$

Note that, the received signal for the second receiver is similar to the first one. For simplicity of notation assume $H' = \left(\sqrt{1-\rho^2}\right)H$ and $\Delta H' = \rho(\Delta H)$. Thus, equation (8) can be rearranged to separate the effect of CSI imperfectness as:

$$\begin{aligned} Y'_1 = (\sqrt{1-\rho^2})\mathrm{Y}_1 + \sqrt{\frac{3P\rho^2}{2}}\Bigg(&\begin{bmatrix} s_{11}^1 & s_{11}^2 \\ -s_{11}^{2*} & s_{11}^{1*} \\ 0 & 0 \end{bmatrix}\frac{A^{-1}}{\|A^{-1}\|}.\Delta H + \begin{bmatrix} s_{21}^1 & s_{21}^2 \\ -s_{21}^{2*} & s_{21}^{1*} \\ 0 & 0 \end{bmatrix}\frac{B^{-1}}{\|B^{-1}\|}.\Delta G \\ &+ \begin{bmatrix} 0 & 0 \\ -s_{12}^{2*} & s_{12}^{1*} \\ s_{12}^1 & s_{12}^2 \end{bmatrix}\frac{H^{-1}}{\|H^{-1}\|}.\Delta H + \begin{bmatrix} 0 & 0 \\ -s_{22}^{2*} & s_{22}^{1*} \\ s_{22}^1 & s_{22}^2 \end{bmatrix}\frac{G^{-1}}{\|G^{-1}\|}.\Delta G\Bigg) + \mathrm{W}'_1 \end{aligned} \tag{9}$$

To rearrange the equation with respect to message signals, conjugating the second timeslot of the received data and reshaping it yields equation (10) where for simplicity of notation we defined:

The equation (10) shows the beamforming error in an imperfect CSI. In relation (10), y_{ij} is transpose of i^{th} row of Y'_i and $\widetilde{w}_1 = vec([w'_{11} \quad w'^{*}_{12} \quad w'_{13}]^T)$ and $\tilde{h}_{ij}$, $\tilde{g}_{ij}$ are entries of $\tilde{H}$ and $\tilde{G}$ which declared in (6) and $\delta\hat{h}_{ij}$, $\delta\hat{g}_{ij}$, $\delta\tilde{h}_{ij}$ and $\delta\tilde{g}_{ij}$ are the entries of defined matrices in (11).

The first term of (10) represents the perfect CSI signals which declared in section 2 and the second term denotes the error signal produced by imperfect CSI.

Thus the perfect CSI signals and imperfect CSI effect on system are separated from each other in the receiver side.

$$\tilde{y}_1 = \mathrm{vec}\begin{bmatrix} y_{11} \\ y_{12}^{*} \\ y_{13} \end{bmatrix} = \sqrt{\frac{3P(1-\rho^2)}{2}} \overbrace{\begin{bmatrix} \tilde{h}_{11} & \tilde{h}_{21} & \tilde{g}_{11} & \tilde{g}_{21} & 0 & 0 & 0 & 0 \\ \tilde{h}_{21}^{*} & -\tilde{h}_{11}^{*} & \tilde{g}_{21}^{*} & -\tilde{g}_{11}^{*} & 0 & 0 & -a & -b \\ 0 & 0 & 0 & 0 & a & b & 0 & 0 \\ \tilde{h}_{12} & \tilde{h}_{22} & \tilde{g}_{12} & \tilde{g}_{22} & 0 & 0 & 0 & 0 \\ \tilde{h}_{22}^{*} & -\tilde{h}_{12}^{*} & \tilde{g}_{22}^{*} & \tilde{g}_{12}^{*} & a & b & 0 & 0 \\ 0 & 0 & 0 & 0 & 0 & 0 & a & b \end{bmatrix}}^{\text{Perfect CSI}} \begin{bmatrix} s_{11}^{1} \\ s_{11}^{2} \\ s_{21}^{1} \\ s_{21}^{2} \\ s_{12}^{1} \\ s_{12}^{2} \\ s_{22}^{1} \\ s_{22}^{2} \end{bmatrix} + \tag{10}$$

$$\sqrt{\frac{3P\rho^2}{2}} \underbrace{\begin{bmatrix} \delta\hat{h}_{11} & \delta\hat{h}_{21} & \delta\hat{g}_{11} & \delta\hat{g}_{21} & 0 & 0 & 0 & 0 \\ \delta\hat{h}_{21}^{*} & -\delta\hat{h}_{11}^{*} & \delta\hat{g}_{21}^{*} & -\delta\hat{g}_{11}^{*} & \delta\tilde{h}_{21}^{*} & -\delta\tilde{h}_{11}^{*} & \delta\tilde{g}_{21}^{*} & -\delta\tilde{g}_{11}^{*} \\ 0 & 0 & 0 & 0 & \delta\tilde{h}_{11} & \delta\tilde{h}_{21} & \delta\tilde{g}_{11} & \delta\tilde{g}_{21} \\ \delta\hat{h}_{12} & \delta\hat{h}_{22} & \delta\hat{g}_{12} & \delta\hat{g}_{22} & 0 & 0 & 0 & 0 \\ \delta\hat{h}_{22}^{*} & -\delta\hat{h}_{12}^{*} & \delta\hat{g}_{22}^{*} & -\delta\hat{g}_{12}^{*} & \delta\tilde{h}_{22}^{*} & -\delta\tilde{h}_{12}^{*} & \delta\tilde{g}_{22}^{*} & -\delta\tilde{g}_{12}^{*} \\ 0 & 0 & 0 & 0 & \delta\tilde{h}_{12} & \delta\tilde{h}_{22} & \delta\tilde{g}_{12} & \delta\tilde{g}_{22} \end{bmatrix}}_{\text{Imperfect CSI}} \begin{bmatrix} s_{11}^{1} \\ s_{11}^{2} \\ s_{21}^{1} \\ s_{21}^{2} \\ s_{12}^{1} \\ s_{12}^{2} \\ s_{22}^{1} \\ s_{22}^{2} \end{bmatrix} + \tilde{w}_1$$

$$\Delta\hat{H} = \frac{A^{-1}}{\|A^{-1}\|}.\Delta H \ , \ \Delta\tilde{H} = \frac{H^{-1}}{\|H^{-1}\|}.\Delta H$$

$$\Delta\hat{G} = \frac{B^{-1}}{\|B^{-1}\|}.\Delta G \ , \ \Delta\tilde{G} = \frac{G^{-1}}{\|G^{-1}\|}.\Delta G \tag{11}$$

3.2. Receiver Error

In the imperfect CSI scenario, the receiver is needed to do two main processes: in the first step interference should be suppressed and in the second step Alamouti decoding should be utilized. We explain these processes in the next two steps:

Step 1. Interference Suppression

Receivers can use timeslots with no desired signal (3, 6 for receiver 1 in equation 10 and 1, 4 for receiver 2 in the similar equation for $\tilde{y}_2$) to cancel the interference in other timeslots which include desired signal. Here, for simplicity, we only consider the first receiver. There are similar equations for the second receiver. Define the variables $\hat{y}_1$ and $\hat{y}_2$ as:

$$\hat{y}_1 = [\tilde{y}_{11} \quad \tilde{y}_{12} + \tilde{y}_{16}]^T$$
$$\hat{y}_2 = [\tilde{y}_{14} \quad \tilde{y}_{15} - \tilde{y}_{13}]^T \tag{12}$$
$$\hat{w}_1 = [\tilde{w}_{11} \quad \tilde{w}_{12} + \tilde{w}_{16}]^T$$
$$\hat{w}_2 = [\tilde{w}_{14} \quad \tilde{w}_{15} - \tilde{w}_{13}]^T$$

where $\tilde{y}_{ij}$ are j^{th} row of matrice $\tilde{y}_i$. By substituting the appropriate terms of (10) in (12) we have the relation (13). The first term of (13) denotes the desired signal for receiver 1 with the assumption of perfect CSI while the second term denotes the error of received signal caused by imperfect CSI at the receiver, and the third term is stands for remained interfering signal caused by imperfect CSI at the transmitter and consequently imperfect beamforming. As it is shown in (13), the imperfect CSI error is separated from desired signal and is divided into two separate terms. However, there is no multiplicative or exponential error term. Thus, the transmission error, caused by imperfect CSI, has a linear form at receiver.

Step 2. Alamouti Decoding

To decode the Alamouti coded signal at the receiver side, for the first step, we should distinguish the desired signals of the first transmitter from the second ones. To declare all received signals, equation (13) can be rearranged as follows:

Desired

$\Delta\hat{H}_1$ Desired signal Error

$$\begin{bmatrix}\hat{\boldsymbol{y}}_{\boldsymbol{1}}\\ \hat{\boldsymbol{y}}_{\boldsymbol{2}}\end{bmatrix}=\sqrt{\frac{\boldsymbol{3P(1-\rho^2)}}{\boldsymbol{2}}}\left(\begin{bmatrix}\tilde{h}_{11} & \tilde{h}_{21}\\ \tilde{h}_{21}^* & -\tilde{h}_{11}^*\\ \tilde{h}_{12} & \tilde{h}_{22}\\ \tilde{h}_{22}^* & -\tilde{h}_{12}^*\end{bmatrix}\begin{bmatrix}s_{11}^1\\ s_{11}^2\end{bmatrix}+\begin{bmatrix}\tilde{g}_{11} & \tilde{g}_{21}\\ \tilde{g}_{21}^* & -\tilde{g}_{11}^*\\ \tilde{g}_{12} & \tilde{g}_{22}\\ \tilde{g}_{22}^* & -\tilde{g}_{12}^*\end{bmatrix}\begin{bmatrix}s_{21}^1\\ s_{21}^2\end{bmatrix}\right)+\sqrt{\frac{\boldsymbol{3P\rho^2}}{\boldsymbol{2}}}\left(\begin{bmatrix}\delta\hat{h}_{11} & \delta\hat{h}_{21}\\ \delta\hat{h}_{21}^* & -\delta\hat{h}_{11}^*\\ \delta\hat{h}_{12} & \delta\hat{h}_{22}\\ \delta\hat{h}_{22}^* & -\delta\hat{h}_{12}^*\end{bmatrix}\begin{bmatrix}s_{11}^1\\ s_{11}^2\end{bmatrix}+\right.$$
$$\begin{bmatrix}\delta\hat{g}_{11} & \delta\hat{g}_{21}\\ \delta\hat{g}_{21}^* & -\delta\hat{g}_{11}^*\\ \delta\hat{g}_{12} & \delta\hat{g}_{22}\\ \delta\hat{g}_{22}^* & -\delta\hat{g}_{12}^*\end{bmatrix}\begin{bmatrix}s_{21}^1\\ s_{21}^2\end{bmatrix}+\begin{bmatrix}0 & 0\\ \delta\tilde{h}_{21}^*+\delta\tilde{h}_{12} & -\delta\tilde{h}_{11}^*+\delta\tilde{h}_{22}\\ 0 & 0\\ \delta\tilde{h}_{22}^*-\delta\tilde{h}_{11} & -\delta\tilde{h}_{12}^*-\delta\tilde{h}_{21}\end{bmatrix}\begin{bmatrix}s_{12}^1\\ s_{12}^2\end{bmatrix}+$$
$$\underbrace{\left.\begin{bmatrix}0 & 0\\ \delta\tilde{g}_{21}^*+\delta\tilde{g}_{12} & -\delta\tilde{g}_{11}^*+\delta\tilde{g}_{22}\\ 0 & 0\\ \delta\tilde{g}_{22}^*-\delta\tilde{g}_{11} & -\delta\tilde{g}_{12}^*-\delta\tilde{g}_{21}\end{bmatrix}\begin{bmatrix}s_{22}^1\\ s_{22}^2\end{bmatrix}\right)}_{\text{Interfering}}+\begin{bmatrix}\hat{\boldsymbol{w}}_{\boldsymbol{1}}\\ \hat{\boldsymbol{w}}_{\boldsymbol{2}}\end{bmatrix} \tag{13}$$

$$\begin{bmatrix}\hat{\boldsymbol{y}}_{\boldsymbol{1}}\\ \hat{\boldsymbol{y}}_{\boldsymbol{2}}\end{bmatrix}=\sqrt{\frac{3P(1-\rho^2)}{2}}\left(\begin{bmatrix}\hat{H}_1\\ \hat{H}_2\end{bmatrix}\begin{bmatrix}s_{11}^1\\ s_{11}^2\end{bmatrix}+\begin{bmatrix}\hat{G}_1\\ \hat{G}_2\end{bmatrix}\begin{bmatrix}s_{21}^1\\ s_{21}^2\end{bmatrix}\right)+\sqrt{\frac{3P\rho^2}{2}}\left(\begin{bmatrix}\Delta\hat{H}_1\\ \Delta\hat{H}_2\end{bmatrix}\begin{bmatrix}s_{11}^1\\ s_{11}^2\end{bmatrix}+\begin{bmatrix}\Delta\hat{G}_1\\ \Delta\hat{G}_2\end{bmatrix}\begin{bmatrix}s_{21}^1\\ s_{21}^2\end{bmatrix}+\begin{bmatrix}\Delta\tilde{H}_1\\ \Delta\tilde{H}_2\end{bmatrix}\begin{bmatrix}s_{12}^1\\ s_{12}^2\end{bmatrix}+\begin{bmatrix}\Delta\tilde{G}_1\\ \Delta\tilde{G}_2\end{bmatrix}\begin{bmatrix}s_{22}^1\\ s_{22}^2\end{bmatrix}\right)+\begin{bmatrix}\hat{\boldsymbol{w}}_{\boldsymbol{1}}\\ \hat{\boldsymbol{w}}_{\boldsymbol{2}}\end{bmatrix} \tag{14}$$

where $\hat{H}_i$, $\hat{G}_i$, $\Delta\hat{H}_i$ and $\Delta\hat{G}_i$,as well as shown in (13), are

$$\hat{H}_i=\begin{bmatrix}\tilde{h}_{1i} & \tilde{h}_{1i}\\ \tilde{h}_{2i}^* & -\tilde{h}_{1i}^*\end{bmatrix},\ \overbrace{\hat{G}_i=}^{\hat{H}}\begin{bmatrix}\tilde{g}_{1i} & \tilde{g}_{1i}\\ \tilde{g}_{2i}^* & -\tilde{g}_{1i}^*\end{bmatrix}$$
$$\Delta\hat{H}_i=\begin{bmatrix}\delta\hat{h}_{1i} & \delta\hat{h}_{2i}\\ \delta\hat{h}_{2i}^* & \delta\hat{h}_{1i}^*\end{bmatrix},\Delta\hat{G}_i=\begin{bmatrix}\delta\hat{g}_{1i} & \delta\hat{g}_{2i}\\ \delta\hat{g}_{2i}^* & \delta\hat{g}_{1i}^*\end{bmatrix} \tag{15}$$

Since CSI is imperfect in the receiver, the decoding matrix is generated as

$$\tilde{G}=V_{21}G \quad , \quad \tilde{H}=V_{11}H \tag{16}$$

Now $\hat{H}_i$ and $\hat{G}_i$ can be obtained from $\tilde{H},\tilde{G}$ at the receiver by (16). We express the process for decoding of desired messages from first transmitter to the first receiver. The desired signal of the second transmitte

$$\overbrace{\frac{\hat{\boldsymbol{G}}_{\boldsymbol{1}}^{\boldsymbol{H}}\hat{\boldsymbol{y}}_{\boldsymbol{1}}}{\|\hat{\boldsymbol{G}}_{\boldsymbol{1}}\|^2}-\frac{\hat{\boldsymbol{G}}_{\boldsymbol{2}}^{\boldsymbol{H}}\hat{\boldsymbol{y}}_{\boldsymbol{2}}}{\|\hat{\boldsymbol{G}}_{\boldsymbol{2}}\|^2}}^{\hat{\boldsymbol{y}}}=\left(\overbrace{\begin{bmatrix}\overset{\hat{H}_1}{\boxed{\frac{\hat{\boldsymbol{G}}_{\boldsymbol{1}}^{\boldsymbol{H}}}{\|\hat{\boldsymbol{G}}_{\boldsymbol{1}}\|^2}}} & -\frac{\hat{\boldsymbol{G}}_{\boldsymbol{2}}^{\boldsymbol{H}}}{\|\hat{\boldsymbol{G}}_{\boldsymbol{2}}\|^2}\end{bmatrix}}^{\hat{G}^{\mathrm{H}}}\begin{bmatrix}\hat{\boldsymbol{y}}_{\boldsymbol{1}}\\ \hat{\boldsymbol{y}}_{\boldsymbol{2}}\end{bmatrix}\right)=\sqrt{\frac{3P(1-\rho^2)}{2}}\left(\begin{bmatrix}\frac{\hat{\boldsymbol{G}}_{\boldsymbol{1}}^{\boldsymbol{H}}}{\|\hat{\boldsymbol{G}}_{\boldsymbol{1}}\|^2} & \overset{\Delta\hat{H}_1}{\boxed{-\frac{\hat{\boldsymbol{G}}_{\boldsymbol{2}}^{\boldsymbol{H}}}{\|\hat{\boldsymbol{G}}_{\boldsymbol{2}}\|^2}}}\end{bmatrix}\overbrace{\begin{bmatrix}\hat{\boldsymbol{H}}_{\boldsymbol{1}}\\ \hat{\boldsymbol{H}}_{\boldsymbol{2}}\end{bmatrix}}^{\hat{H}}\begin{bmatrix}s_{11}^1\\ s_{11}^2\end{bmatrix}\right)+$$
$$\sqrt{\frac{3P\rho^2}{2}}\left(\begin{bmatrix}\frac{\hat{\boldsymbol{G}}_{\boldsymbol{1}}^{\boldsymbol{H}}}{\|\hat{\boldsymbol{G}}_{\boldsymbol{1}}\|^2} & -\frac{\hat{\boldsymbol{G}}_{\boldsymbol{2}}^{\boldsymbol{H}}}{\|\hat{\boldsymbol{G}}_{\boldsymbol{2}}\|^2}\end{bmatrix}\begin{bmatrix}\Delta\hat{\boldsymbol{H}}_{\boldsymbol{1}}\\ \Delta\hat{\boldsymbol{H}}_{\boldsymbol{2}}\end{bmatrix}\begin{bmatrix}s_{11}^1\\ s_{11}^2\end{bmatrix}+\begin{bmatrix}\frac{\hat{\boldsymbol{G}}_{\boldsymbol{1}}^{\boldsymbol{H}}}{\|\hat{\boldsymbol{G}}_{\boldsymbol{1}}\|^2} & -\frac{\hat{\boldsymbol{G}}_{\boldsymbol{2}}^{\boldsymbol{H}}}{\|\hat{\boldsymbol{G}}_{\boldsymbol{2}}\|^2}\end{bmatrix}\begin{bmatrix}\Delta\hat{\boldsymbol{G}}_{\boldsymbol{1}}\\ \Delta\hat{\boldsymbol{G}}_{\boldsymbol{2}}\end{bmatrix}\begin{bmatrix}s_{21}^1\\ s_{21}^2\end{bmatrix}+\right. \tag{17}$$
$$\left.\begin{bmatrix}\frac{\hat{\boldsymbol{G}}_{\boldsymbol{1}}^{\boldsymbol{H}}}{\|\hat{\boldsymbol{G}}_{\boldsymbol{1}}\|^2} & -\frac{\hat{\boldsymbol{G}}_{\boldsymbol{2}}^{\boldsymbol{H}}}{\|\hat{\boldsymbol{G}}_{\boldsymbol{2}}\|^2}\end{bmatrix}\begin{bmatrix}\Delta\tilde{\boldsymbol{H}}_{\boldsymbol{1}}\\ \Delta\tilde{\boldsymbol{H}}_{\boldsymbol{2}}\end{bmatrix}\begin{bmatrix}s_{12}^1\\ s_{12}^2\end{bmatrix}+\begin{bmatrix}\frac{\hat{\boldsymbol{G}}_{\boldsymbol{1}}^{\boldsymbol{H}}}{\|\hat{\boldsymbol{G}}_{\boldsymbol{1}}\|^2} & -\frac{\hat{\boldsymbol{G}}_{\boldsymbol{2}}^{\boldsymbol{H}}}{\|\hat{\boldsymbol{G}}_{\boldsymbol{2}}\|^2}\end{bmatrix}\begin{bmatrix}\Delta\tilde{\boldsymbol{G}}_{\boldsymbol{1}}\\ \Delta\tilde{\boldsymbol{G}}_{\boldsymbol{2}}\end{bmatrix}\begin{bmatrix}s_{22}^1\\ s_{22}^2\end{bmatrix}\right)+\begin{bmatrix}\frac{\hat{\boldsymbol{G}}_{\boldsymbol{1}}^{\boldsymbol{H}}}{\|\hat{\boldsymbol{G}}_{\boldsymbol{1}}\|^2} & -\frac{\hat{\boldsymbol{G}}_{\boldsymbol{2}}^{\boldsymbol{H}}}{\|\hat{\boldsymbol{G}}_{\boldsymbol{2}}\|^2}\end{bmatrix}\begin{bmatrix}\hat{\boldsymbol{w}}_{\boldsymbol{1}}\\ \hat{\boldsymbol{w}}_{\boldsymbol{2}}\end{bmatrix}$$

can be obtained similarly. To distinguish the desired signals from the first transmitter, we calculate equation (17).

Defining $\hat{\boldsymbol{y}}=\frac{\hat{\mathbf{G}}_{\mathbf{1}}^{\mathbf{H}}\hat{\mathbf{y}}_{\mathbf{1}}}{\|\hat{\mathbf{G}}_{\mathbf{1}}\|^2}-\frac{\hat{\mathbf{G}}_{\mathbf{2}}^{\mathbf{H}}\hat{\mathbf{y}}_{\mathbf{2}}}{\|\hat{\mathbf{G}}_{\mathbf{2}}\|^2}$, $\hat{\boldsymbol{G}}^{\boldsymbol{H}}=\begin{bmatrix}\frac{\hat{\boldsymbol{G}}_{\boldsymbol{1}}^{\boldsymbol{H}}}{\|\hat{\boldsymbol{G}}_{\boldsymbol{1}}\|^2} & -\frac{\hat{\boldsymbol{G}}_{\boldsymbol{2}}^{\boldsymbol{H}}}{\|\hat{\boldsymbol{G}}_{\boldsymbol{2}}\|^2}\end{bmatrix}$ and $\hat{\boldsymbol{H}}=\begin{bmatrix}\hat{\boldsymbol{H}}_{\boldsymbol{1}}\\ \hat{\boldsymbol{H}}_{\boldsymbol{2}}\end{bmatrix}$, we can simplify the expression as:

$$\hat{\boldsymbol{y}}=\sqrt{\frac{3P(1-\rho^2)}{2}}\left(\hat{\boldsymbol{G}}^{\boldsymbol{H}}\hat{\boldsymbol{H}}\begin{bmatrix}s_{11}^1\\ s_{11}^2\end{bmatrix}\right)+\sqrt{\frac{3P\rho^2}{2}}\left(\hat{\boldsymbol{G}}^{\boldsymbol{H}}\begin{bmatrix}\Delta\hat{\boldsymbol{H}}_{\boldsymbol{1}}\\ \Delta\hat{\boldsymbol{H}}_{\boldsymbol{2}}\end{bmatrix}\begin{bmatrix}s_{11}^1\\ s_{11}^2\end{bmatrix}+\hat{\boldsymbol{G}}^{\boldsymbol{H}}\begin{bmatrix}\Delta\hat{\boldsymbol{G}}_{\boldsymbol{1}}\\ \Delta\hat{\boldsymbol{G}}_{\boldsymbol{2}}\end{bmatrix}\begin{bmatrix}s_{21}^1\\ s_{21}^2\end{bmatrix}+\hat{\boldsymbol{G}}^{\boldsymbol{H}}\begin{bmatrix}\Delta\tilde{\boldsymbol{H}}_{\boldsymbol{1}}\\ \Delta\tilde{\boldsymbol{H}}_{\boldsymbol{2}}\end{bmatrix}\begin{bmatrix}s_{12}^1\\ s_{12}^2\end{bmatrix}+\hat{\boldsymbol{G}}^{\boldsymbol{H}}\begin{bmatrix}\Delta\tilde{\boldsymbol{G}}_{\boldsymbol{1}}\\ \Delta\tilde{\boldsymbol{G}}_{\boldsymbol{2}}\end{bmatrix}\begin{bmatrix}s_{22}^1\\ s_{22}^2\end{bmatrix}\right)+\hat{\boldsymbol{G}}^{\boldsymbol{H}}\begin{bmatrix}\hat{\boldsymbol{w}}_{\boldsymbol{1}}\\ \hat{\boldsymbol{w}}_{\boldsymbol{2}}\end{bmatrix} \tag{18}$$

Now, the signal can be decoded by Alamouti decoder as follows:

$$\hat{\boldsymbol{s}}=\hat{\boldsymbol{H}}^{\boldsymbol{H}}\hat{\boldsymbol{G}}\,\hat{\boldsymbol{y}}=\sqrt{\frac{3P(1-\rho^2)}{2}}\left(\hat{\boldsymbol{H}}^{\boldsymbol{H}}\hat{\boldsymbol{G}}\,\hat{\boldsymbol{G}}^{\boldsymbol{H}}\hat{\boldsymbol{H}}\begin{bmatrix}s_{11}^1\\ s_{11}^2\end{bmatrix}\right)+\sqrt{\frac{3P\rho^2}{2}}\hat{\boldsymbol{H}}^{\boldsymbol{H}}\hat{\boldsymbol{G}}\left(\hat{\boldsymbol{G}}^{\boldsymbol{H}}\begin{bmatrix}\Delta\hat{\boldsymbol{H}}_{\boldsymbol{1}}\\ \Delta\hat{\boldsymbol{H}}_{\boldsymbol{2}}\end{bmatrix}\begin{bmatrix}s_{11}^1\\ s_{11}^2\end{bmatrix}+\hat{\boldsymbol{G}}^{\boldsymbol{H}}\begin{bmatrix}\Delta\hat{\boldsymbol{G}}_{\boldsymbol{1}}\\ \Delta\hat{\boldsymbol{G}}_{\boldsymbol{2}}\end{bmatrix}\begin{bmatrix}s_{21}^1\\ s_{21}^2\end{bmatrix}+\hat{\boldsymbol{G}}^{\boldsymbol{H}}\begin{bmatrix}\Delta\tilde{\boldsymbol{H}}_{\boldsymbol{1}}\\ \Delta\tilde{\boldsymbol{H}}_{\boldsymbol{2}}\end{bmatrix}\begin{bmatrix}s_{12}^1\\ s_{12}^2\end{bmatrix}+\hat{\boldsymbol{G}}^{\boldsymbol{H}}\begin{bmatrix}\Delta\tilde{\boldsymbol{G}}_{\boldsymbol{1}}\\ \Delta\tilde{\boldsymbol{G}}_{\boldsymbol{2}}\end{bmatrix}\begin{bmatrix}s_{22}^1\\ s_{22}^2\end{bmatrix}\right)+\hat{\boldsymbol{H}}^{\boldsymbol{H}}\hat{\boldsymbol{G}}\,\hat{\boldsymbol{G}}^{\boldsymbol{H}}\begin{bmatrix}\hat{\boldsymbol{w}}_{\boldsymbol{1}}\\ \hat{\boldsymbol{w}}_{\boldsymbol{2}}\end{bmatrix} \tag{19}$$

where $\hat{\boldsymbol{s}}$ is the decoded signal vector. Now we can detect the transmitted signal with a Maximum Likelihood (ML) detector as:

$$s_{11}^k=arg\ \max_{s}\hat{s}_k.s\ ;\quad k=1,2 \tag{20}$$

where $\hat{s}_k$ is the k^{th} component of $\hat{\boldsymbol{s}}$ .The symbol s_{12}^k can be detected similarly.

The first term of the left side of (19) is the desired signal from the first transmitter to the first receiver, which decodes s_{11}^1, s_{11}^2 while the other terms caused by imperfect CSI. The Second and third term are distorted copies of desired signal from first and second transmitter, fourth and fifth term are misaligned interference.

Thus, terms 2 to 5 of (19) will operate as noise and cause SINR reduction and increase the BER of system. The increase of BER growth linearly related to CSI error covariance because of multiplication of channel coefficient matrices to error matrices. Since error entries are i.i.d., the covariance matrix is identical to CSI error variance. Thus, benefit the Alamouti coding together with the IA is feasible under the imperfect CSI scenario, but performance of system will decrease linearly by increasing the CSI error variance.

According to (19), the received SINR at detector of receiver, which is declared in (20), can be calculated as (21):

$$SINR = \frac{\frac{3P(1-\rho^2)}{2}\, Tr(\widehat{\boldsymbol{H}}^{\mathrm{H}}\widehat{\boldsymbol{G}}\,\widehat{\boldsymbol{G}}^{\mathrm{H}}\widehat{\boldsymbol{H}})}{\frac{3P\rho^2}{2} Tr\left(\widehat{\boldsymbol{H}}^{\mathrm{H}}\widehat{\boldsymbol{G}}\left(\widehat{\boldsymbol{G}}^{\mathrm{H}}\left(\begin{bmatrix}\Delta\widehat{\boldsymbol{H}}_1\\ \Delta\widehat{\boldsymbol{H}}_2\end{bmatrix}+\begin{bmatrix}\Delta\widehat{\boldsymbol{G}}_1\\ \Delta\widehat{\boldsymbol{G}}_2\end{bmatrix}+\begin{bmatrix}\Delta\widetilde{\boldsymbol{H}}_1\\ \Delta\widetilde{\boldsymbol{H}}_2\end{bmatrix}+\begin{bmatrix}\Delta\widetilde{\boldsymbol{G}}_1\\ \Delta\widetilde{\boldsymbol{G}}_2\end{bmatrix}\right)\right)\right)+Tr\left(\widehat{\boldsymbol{H}}^{\mathrm{H}}\widehat{\boldsymbol{G}}\,\widehat{\boldsymbol{G}}^{\mathrm{H}}\begin{bmatrix}\widehat{\boldsymbol{w}}_1\\ \widehat{\boldsymbol{w}}_2\end{bmatrix}\right)} \tag{21}$$

where $Tr(.)$ stands for Trace operator. As it is shown in (21), increment in transmit power will increase residual interference and distorted signal at the denominator of SINR equation. The received SINR, in high SNR regime, can be calculated as:

$$\lim_{P\to\infty} SINR \cong \frac{(1-\rho^2)\ Tr(\widehat{\boldsymbol{H}}^{\mathrm{H}}\widehat{\boldsymbol{G}}\,\widehat{\boldsymbol{G}}^{\mathrm{H}}\widehat{\boldsymbol{H}})}{\rho^2\, Tr\left(\widehat{\boldsymbol{H}}^{\mathrm{H}}\widehat{\boldsymbol{G}}\left(\widehat{\boldsymbol{G}}^{\mathrm{H}}\left(\begin{bmatrix}\Delta\widehat{\boldsymbol{H}}_1\\ \Delta\widehat{\boldsymbol{H}}_2\end{bmatrix}+\begin{bmatrix}\Delta\widehat{\boldsymbol{G}}_1\\ \Delta\widehat{\boldsymbol{G}}_2\end{bmatrix}+\begin{bmatrix}\Delta\widetilde{\boldsymbol{H}}_1\\ \Delta\widetilde{\boldsymbol{H}}_2\end{bmatrix}+\begin{bmatrix}\Delta\widetilde{\boldsymbol{G}}_1\\ \Delta\widetilde{\boldsymbol{G}}_2\end{bmatrix}\right)\right)\right)} \tag{22}$$

Thus, the SINR is proportional to $\frac{(1-\rho^2)}{\rho^2}$ at high SNR regime and the effect of imperfect CSI will increase with SNR. Note that the SINR value in high SNR region is not related to P. Computer simulations will clarify this result.

4. System performance improvement with Power Allocation

Power Allocation (PA) is a simple way in MIMO systems to increase the system performance during the channel coefficients variations. Thus, we can use PA between two TX antennas of each transmitter and improve the received signal BER at the receiver side. By defining $\sqrt{x_1} = p_1$, $\sqrt{1-x_1} = p_2$, $\sqrt{x_2} = p_3$ and $\sqrt{1-x_2} = p_4$, we rearrange (3) , (4) as :

$$\mathrm{X}_1^p = \sqrt{\frac{3P}{1}}\left(\begin{bmatrix} s_{11}^1 & s_{11}^2\\ -s_{11}^{2*} & s_{11}^{1*}\\ 0 & 0\end{bmatrix}\begin{bmatrix}p_1 & 0\\ 0 & p_2\end{bmatrix}\boldsymbol{V}_{11} + \begin{bmatrix} 0 & 0\\ -s_{12}^{2*} & s_{12}^{1}\\ s_{12}^1 & s_{12}^2\end{bmatrix}\begin{bmatrix}p_1 & 0\\ 0 & p_2\end{bmatrix}\boldsymbol{V}_{12}\right) \tag{23}$$

$$\mathrm{X}_1^p = \sqrt{\frac{3P}{1}}\left(\begin{bmatrix} s_{11}^1 & s_{11}^2\\ -s_{11}^{2*} & s_{11}^{1*}\\ 0 & 0\end{bmatrix}\begin{bmatrix}p_1 & 0\\ 0 & p_2\end{bmatrix}\boldsymbol{V}_{11} + \begin{bmatrix} 0 & 0\\ -s_{12}^{2*} & s_{12}^{1}\\ s_{12}^1 & s_{12}^2\end{bmatrix}\begin{bmatrix}p_1 & 0\\ 0 & p_2\end{bmatrix}\boldsymbol{V}_{12}\right)$$

Replacing X_1^p and X_2^p in (6) and rewriting equations (7) to (12), equation (13) can be expressed as (24).

As it is shown in (24), to suppress interference terms from received signal (term 2, 3 of equation (24)) we should consider two following conditions:

- Power allocation ratio for both transmitters should be identical, i.e. $p_1 = p_3$ and $p_2 = p_4$.
- Receivers should know power allocation values, i.e. p_1, p_2, p_3 and p_4.

$$\begin{bmatrix}\widehat{\boldsymbol{y}}_1\\ \widehat{\boldsymbol{y}}_2\end{bmatrix} = \sqrt{\frac{3P(1-\rho^2)}{1}}\left(\begin{bmatrix} p_1\tilde{h}_{11} & p_2\tilde{h}_{21}\\ p_2\tilde{h}_{21}^* & -p_1\tilde{h}_{11}^*\\ p_1\tilde{h}_{12} & p_2\tilde{h}_{22}\\ p_2\tilde{h}_{22}^* & -p_1\tilde{h}_{12}^*\end{bmatrix}\begin{bmatrix}s_{11}^1\\ s_{11}^2\end{bmatrix} + \begin{bmatrix} p_3\tilde{g}_{11} & p_4\tilde{g}_{21}\\ p_4\tilde{g}_{21}^* & -p_3\tilde{g}_{11}^*\\ p_3\tilde{g}_{12} & p_4\tilde{g}_{22}\\ p_4\tilde{g}_{22}^* & -p_3\tilde{g}_{12}^*\end{bmatrix}\begin{bmatrix}s_{21}^1\\ s_{21}^2\end{bmatrix} + \begin{bmatrix} 0 & 0\\ a(p_2-p_1) & b(p_4-p_3)\\ 0 & 0\\ 0 & 0\end{bmatrix}\begin{bmatrix}s_{12}^2\\ s_{22}^2\end{bmatrix} + \begin{bmatrix} 0 & 0\\ 0 & 0\\ 0 & 0\\ a(p_2-p_1) & b(p_4-p_3)\end{bmatrix}\begin{bmatrix}s_{12}^1\\ s_{22}^1\end{bmatrix}\right) +$$

$$\sqrt{\frac{3P\rho^2}{2}}\left(\begin{bmatrix} p_1\delta\hat{h}_{11} & p_2\delta\hat{h}_{21}\\ p_2\delta\hat{h}_{21}^* & -p_1\delta\hat{h}_{11}^*\\ p_1\delta\hat{h}_{12} & p_2\delta\hat{h}_{22}\\ p_2\delta\hat{h}_{22}^* & -p_1\delta\hat{h}_{12}^*\end{bmatrix}\begin{bmatrix}s_{11}^1\\ s_{11}^2\end{bmatrix} + \begin{bmatrix} p_3\delta\hat{g}_{11} & p_4\delta\hat{g}_{21}\\ p_4\delta\hat{g}_{21}^* & -p_3\delta\hat{g}_{11}^*\\ p_3\delta\hat{g}_{12} & p_4\delta\hat{g}_{22}\\ p_4\delta\hat{g}_{22}^* & -p_3\delta\hat{g}_{12}^*\end{bmatrix}\begin{bmatrix}s_{21}^1\\ s_{21}^2\end{bmatrix} + \begin{bmatrix} 0 & 0\\ p_2\delta\tilde{h}_{21}^* + p_1\delta\tilde{h}_{12} & -p_1\delta\tilde{h}_{11}^* + p_2\delta\tilde{h}_{22}\\ 0 & 0\\ p_2\delta\tilde{h}_{22}^* - p_1\delta\tilde{h}_{11} & -p_1\delta\tilde{h}_{12}^* - p_2\delta\tilde{h}_{21}\end{bmatrix}\begin{bmatrix}s_{12}^1\\ s_{12}^2\end{bmatrix} + \begin{bmatrix} 0 & 0\\ p_4\delta\tilde{g}_{21}^* + p_3\delta\tilde{g}_{12} & -p_3\delta\tilde{g}_{11}^* + p_4\delta\tilde{g}_{22}\\ 0 & 0\\ p_4\delta\tilde{g}_{22}^* - p_3\delta\tilde{g}_{11} & -p_3\delta\tilde{g}_{12}^* - p_4\delta\tilde{g}_{21}\end{bmatrix}\begin{bmatrix}s_{22}^1\\ s_{22}^2\end{bmatrix}\right) + \begin{bmatrix}\widehat{\boldsymbol{w}}_1\\ \widehat{\boldsymbol{w}}_2\end{bmatrix}$$

(24)

Thus we can replace (12) with its corresponding values as,

$$\hat{\boldsymbol{y}}_{\boldsymbol{1}} = \begin{bmatrix}\tilde{y}_{11} & \tilde{y}_{12} + \frac{p_1}{p_2}\tilde{y}_{16}\end{bmatrix}^T$$
$$\hat{\boldsymbol{y}}_{\boldsymbol{2}} = \begin{bmatrix}\tilde{y}_{14} & \tilde{y}_{15} - \frac{p_2}{p_1}\tilde{y}_{13}\end{bmatrix}^T$$
$$\hat{\boldsymbol{w}}_{\boldsymbol{1}} = \begin{bmatrix}\tilde{w}_{11} & \tilde{w}_{12} + \frac{p_1}{p_2}\tilde{w}_{16}\end{bmatrix}^T$$
$$\hat{\boldsymbol{w}}_{\boldsymbol{2}} = \begin{bmatrix}\tilde{w}_{14} & \tilde{w}_{15} - \frac{p_2}{p_1}\tilde{w}_{13}\end{bmatrix}^T \tag{25}$$

Now, (24) can be simplified as (26).

Thus, the resulted SINR with PA can be calculated as (27) where $\widehat{H}^p$, $\widehat{G}^p$, $\widehat{H}_i^p$, $\widehat{G}_i^p$, $\Delta\widehat{H}_i^p$, $\Delta\widehat{G}_i^p$, $\Delta\widetilde{H}_i^p$ and $\Delta\widetilde{G}_i^p$ are rearranged versions of $\widehat{H}$, $\widehat{G}$, $\widehat{H}_i$, $\widehat{G}_i$, $\Delta\widehat{H}_i$, $\Delta\widehat{G}_i$, $\Delta\widetilde{H}_i$ and $\Delta\widetilde{G}_i$ in (15) to (20) due to power allocation strategy.

Unfortunately, finding the best PA ratio to maximize the PA SINR of (27) is not possible for us. Thus, we used a brute-force search method to finding the best PA value for each channel ensembles to declare the efficiency of the proposed PA in imperfect scenario. Simulation results in section VI shows significant improvement in BER of system due to PA.

$$\begin{bmatrix}\hat{y}_1\\ \hat{y}_2\end{bmatrix} = \sqrt{\frac{3P(1-\rho^2)}{1}}\left(\begin{bmatrix}p_1\tilde{h}_{11} & p_2\tilde{h}_{21}\\ p_2\tilde{h}_{21}^* & -p_1\tilde{h}_{11}^*\\ p_1\tilde{h}_{12} & p_2\tilde{h}_{22}\\ p_2\tilde{h}_{22}^* & -p_1\tilde{h}_{12}^*\end{bmatrix}\begin{bmatrix}s_{11}^1\\ s_{11}^2\end{bmatrix} + \begin{bmatrix}p_1\tilde{g}_{11} & p_2\tilde{g}_{21}\\ p_2\tilde{g}_{21}^* & -p_1\tilde{g}_{11}^*\\ p_1\tilde{g}_{12} & p_2\tilde{g}_{22}\\ p_2\tilde{g}_{22}^* & -p_1\tilde{g}_{12}^*\end{bmatrix}\begin{bmatrix}s_{21}^1\\ s_{21}^2\end{bmatrix}\right) + \sqrt{\frac{3P\rho^2}{2}}\left(\begin{bmatrix}p_1\delta\hat{h}_{11} & p_2\delta\hat{h}_{21}\\ p_2\delta\hat{h}_{21}^* & -p_1\delta\hat{h}_{11}^*\\ p_1\delta\hat{h}_{12} & p_2\delta\hat{h}_{22}\\ p_2\delta\hat{h}_{22}^* & -p_1\delta\hat{h}_{12}^*\end{bmatrix}\begin{bmatrix}s_{11}^1\\ s_{11}^2\end{bmatrix} + \right.$$
$$\begin{bmatrix}p_1\delta\hat{g}_{11} & p_2\delta\hat{g}_{21}\\ p_2\delta\hat{g}_{21}^* & -p_1\delta\hat{g}_{11}^*\\ p_1\delta\hat{g}_{12} & p_2\delta\hat{g}_{22}\\ p_2\delta\hat{g}_{22}^* & -p_1\delta\hat{g}_{12}^*\end{bmatrix}\begin{bmatrix}s_{21}^1\\ s_{21}^2\end{bmatrix} + \begin{bmatrix}0 & 0\\ p_2\delta\tilde{h}_{21}^* + \frac{p_1^2}{p_2}\delta\tilde{h}_{12} & -p_1\delta\tilde{h}_{11}^* + p_1\delta\tilde{h}_{22}\\ 0 & 0\\ p_2\delta\tilde{h}_{22}^* - p_2\delta\tilde{h}_{11} & -p_1\delta\tilde{h}_{12}^* - \frac{p_2^2}{p_1}\delta\tilde{h}_{21}\end{bmatrix}\begin{bmatrix}s_{12}^1\\ s_{12}^2\end{bmatrix} +$$
$$\left.\begin{bmatrix}0 & 0\\ p_2\delta\tilde{g}_{21}^* + \frac{p_1^2}{p_2}\delta\tilde{g}_{12} & -p_1\delta\tilde{g}_{11}^* + p_1\delta\tilde{g}_{22}\\ 0 & 0\\ p_2\delta\tilde{g}_{22}^* - p_2\delta\tilde{g}_{11} & -p_1\delta\tilde{g}_{12}^* - \frac{p_1^2}{p_2}\delta\tilde{g}_{21}\end{bmatrix}\begin{bmatrix}s_{22}^1\\ s_{22}^2\end{bmatrix}\right) + \begin{bmatrix}\hat{w}_1\\ \hat{w}_2\end{bmatrix} \tag{26}$$

$$SINR^p = \frac{\frac{3P(1-\rho^2)}{2}\; Tr\left(\widehat{\boldsymbol{H}}^{\boldsymbol{p}^{\boldsymbol{H}}}\widehat{\boldsymbol{G}}^{\boldsymbol{p}}\widehat{\boldsymbol{G}}^{\boldsymbol{p}^{\boldsymbol{H}}}\widehat{\boldsymbol{H}}^{\boldsymbol{p}}\right)}{\frac{3P\rho^2}{2}\; Tr\left(\widehat{\boldsymbol{H}}^{\boldsymbol{p}^{\boldsymbol{H}}}\widehat{\boldsymbol{G}}^{\boldsymbol{p}}\left(\widehat{\boldsymbol{G}}^{\boldsymbol{p}^{\boldsymbol{H}}}\left(\begin{bmatrix}\Delta\widehat{\boldsymbol{H}}_{\boldsymbol{1}}^{\boldsymbol{p}}\\ \Delta\widehat{\boldsymbol{H}}_{\boldsymbol{2}}^{\boldsymbol{p}}\end{bmatrix} + \begin{bmatrix}\Delta\widehat{\boldsymbol{G}}_{\boldsymbol{1}}^{\boldsymbol{p}}\\ \Delta\widehat{\boldsymbol{G}}_{\boldsymbol{2}}^{\boldsymbol{p}}\end{bmatrix} + \begin{bmatrix}\Delta\widetilde{\boldsymbol{H}}_{\boldsymbol{1}}^{\boldsymbol{p}}\\ \Delta\widetilde{\boldsymbol{H}}_{\boldsymbol{2}}^{\boldsymbol{p}}\end{bmatrix} + \begin{bmatrix}\Delta\widetilde{\boldsymbol{G}}_{\boldsymbol{1}}^{\boldsymbol{p}}\\ \Delta\widetilde{\boldsymbol{G}}_{\boldsymbol{2}}^{\boldsymbol{p}}\end{bmatrix}\right)\right)\right) + Tr\left(\widehat{\boldsymbol{H}}^{\boldsymbol{p}^{\boldsymbol{H}}}\widehat{\boldsymbol{G}}^{\boldsymbol{p}}\widehat{\boldsymbol{G}}^{\boldsymbol{p}^{\boldsymbol{H}}}\begin{bmatrix}\widehat{\boldsymbol{w}}_{\boldsymbol{1}}\\ \widehat{\boldsymbol{w}}_{\boldsymbol{2}}\end{bmatrix}\right)} \tag{27}$$

5. System performance improvement with Constellation Rotation

Constellation Rotation (CR) is first introduced in terms of space diversity in [25]. At the first time, CR is used to overcome fading effects on wireless communications systems with PSK and QAM modulation in [26], [27]. Then researches in [28-30] showed that it can be used to improve system performance with imperfect CSI. CR is used for Alamouti coding system in fading channel [31] and also applied in [24] to reduce the desired SNR in a MIMO system. Figure (2) illustrates how CR improves system performance in imperfect CSI scenario. If we consider the CSI error as a distortion in channel space domain, CR tries to rotate the signal constellations to compensate the effect of this distortion on each constellation's space.

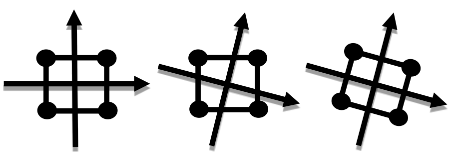

(a) (b) (c)

Fig. 2. QPSK constellation form for a) Perfect CSI, b) Imperfect CSI without CR, c) imperfect CSI with CR

Benefit the CR in the illustrated system of figure (1), transmit signals can be rearranged as follows:

$$\begin{aligned}&[\, b_{11}^2\; b_{12}^1\; b_{12}^2\; b_{21}^1\; b_{21}^2\; b_{22}^1\; b_{22}^2]\\ &\quad = [s_{11}^1\; s_{11}^2\; s_{12}^1\; s_{12}^2\; s_{21}^1\; s_{21}^2\; s_{22}^1\; s_{22}^2] * \exp(j\theta)\end{aligned} \tag{28}$$

where s_{ij}^k are transmitted symbols which defined in (3), (4) and θ is rotation angle. It is clear that all the equations (3) to (17) for b_{ij}^k are the same as s_{ij}^k. Thus the equation (18) can be rearranged as (29):

$$\hat{\boldsymbol{y}} = \sqrt{\frac{3P(1-\rho^2)}{2}}\left(\hat{\boldsymbol{G}}^{\mathrm{H}}\hat{\boldsymbol{H}}\begin{bmatrix}s_{11}^1\\ s_{11}^2\end{bmatrix}\exp(j\theta)\right) + \sqrt{\frac{3P\rho^2}{2}}\left(\hat{\boldsymbol{G}}^{\mathrm{H}}\begin{bmatrix}\Delta\hat{\boldsymbol{H}}_1\\ \Delta\hat{\boldsymbol{H}}_2\end{bmatrix}\begin{bmatrix}s_{11}^1\\ s_{11}^2\end{bmatrix}\exp(j\theta) + \hat{\boldsymbol{G}}^{\mathrm{H}}\begin{bmatrix}\Delta\hat{\boldsymbol{G}}_1\\ \Delta\hat{\boldsymbol{G}}_2\end{bmatrix}\begin{bmatrix}s_{21}^1\\ s_{21}^2\end{bmatrix}\exp(j\theta) + \hat{\boldsymbol{G}}^{\mathrm{H}}\begin{bmatrix}\Delta\tilde{\boldsymbol{H}}_1\\ \Delta\tilde{\boldsymbol{H}}_2\end{bmatrix}\begin{bmatrix}s_{12}^1\\ s_{12}^2\end{bmatrix}\exp(j\theta) + \hat{\boldsymbol{G}}^{\mathrm{H}}\begin{bmatrix}\Delta\tilde{\boldsymbol{G}}_1\\ \Delta\tilde{\boldsymbol{G}}_2\end{bmatrix}\begin{bmatrix}s_{22}^1\\ s_{22}^2\end{bmatrix}\exp(j\theta)\right) + \hat{\boldsymbol{G}}^{\mathrm{H}}\begin{bmatrix}\hat{\boldsymbol{w}}_1\\ \hat{\boldsymbol{w}}_2\end{bmatrix} \quad (29)$$

Thus, the decoding process at the receiver can be expressed as:

$$\begin{bmatrix}\hat{s}_{11}^1\\ \hat{s}_{11}^2\end{bmatrix} = \hat{\boldsymbol{H}}^{\mathrm{H}}\hat{\boldsymbol{G}}\,\hat{\boldsymbol{y}} = \sqrt{\frac{3P(1-\rho^2)}{2}}\left(\hat{\boldsymbol{H}}^{\mathrm{H}}\hat{\boldsymbol{G}}\,\hat{\boldsymbol{G}}^{\mathrm{H}}\hat{\boldsymbol{H}}\begin{bmatrix}s_{11}^1\\ s_{11}^2\end{bmatrix}\exp(j\theta)\right) + \sqrt{\frac{3P\rho^2}{2}}\hat{\boldsymbol{H}}^{\mathrm{H}}\hat{\boldsymbol{G}}\left(\hat{\boldsymbol{G}}^{\mathrm{H}}\left(\begin{bmatrix}\Delta\hat{\boldsymbol{H}}_1\\ \Delta\hat{\boldsymbol{H}}_2\end{bmatrix}\begin{bmatrix}s_{11}^1\\ s_{11}^2\end{bmatrix} + \begin{bmatrix}\Delta\hat{\boldsymbol{G}}_1\\ \Delta\hat{\boldsymbol{G}}_2\end{bmatrix}\begin{bmatrix}s_{21}^1\\ s_{21}^2\end{bmatrix} + \begin{bmatrix}\Delta\tilde{\boldsymbol{H}}_1\\ \Delta\tilde{\boldsymbol{H}}_2\end{bmatrix}\begin{bmatrix}s_{12}^1\\ s_{12}^2\end{bmatrix} + \begin{bmatrix}\Delta\tilde{\boldsymbol{G}}_1\\ \Delta\tilde{\boldsymbol{G}}_2\end{bmatrix}\begin{bmatrix}s_{22}^1\\ s_{22}^2\end{bmatrix}\right)\exp(j\theta)\right) + \hat{\boldsymbol{H}}^{\mathrm{H}}\hat{\boldsymbol{G}}\,\hat{\boldsymbol{G}}^{\mathrm{H}}\begin{bmatrix}\hat{\boldsymbol{w}}_1\\ \hat{\boldsymbol{w}}_2\end{bmatrix} \quad (30)$$

Finally, the rotated constellation should be rearranged to its original form at the ML detector as:

$$s_{11}^k = \arg\max_{s} \hat{s}_{11}^k \exp(-j\theta) \quad , \qquad k = 1,2 \quad (31)$$

Note that, the first part of the right hand side of (30) is the perfect CSI received signals, the second part shows the Imperfect CSI effect and third part is related to noise. Thus, the purpose of CR is to minimize the second part as interference term in (32):

$$\boldsymbol{Ix}_{11}^{R} = \sqrt{\frac{3P\rho^2}{2}}\hat{\boldsymbol{H}}^{\mathrm{H}}\hat{\boldsymbol{G}}\left(\hat{\boldsymbol{G}}^{\mathrm{H}}\left(\begin{bmatrix}\Delta\hat{\boldsymbol{H}}_1\\ \Delta\hat{\boldsymbol{H}}_2\end{bmatrix}\begin{bmatrix}s_{11}^1\\ s_{11}^2\end{bmatrix} + \begin{bmatrix}\Delta\hat{\boldsymbol{G}}_1\\ \Delta\hat{\boldsymbol{G}}_2\end{bmatrix}\begin{bmatrix}s_{21}^1\\ s_{21}^2\end{bmatrix} + \begin{bmatrix}\Delta\tilde{\boldsymbol{H}}_1\\ \Delta\tilde{\boldsymbol{H}}_2\end{bmatrix}\begin{bmatrix}s_{12}^1\\ s_{12}^2\end{bmatrix} + \begin{bmatrix}\Delta\tilde{\boldsymbol{G}}_1\\ \Delta\tilde{\boldsymbol{G}}_2\end{bmatrix}\begin{bmatrix}s_{22}^1\\ s_{22}^2\end{bmatrix}\right)\exp(j\theta)\right) \quad (32)$$

The equation (32) can be denoted as the cost function. The purpose of the CR is to minimize it's power by finding the optimal rotation angle as:

$$\theta_{opt} = \arg\min_{\theta} Tr\left(E\left(\left(\boldsymbol{Ix}_{11}^{R}\right)^{H}.\boldsymbol{Ix}_{11}^{R}\right)\right) \quad (33)$$

Since finding a closed form for θ_{opt} is so complicated, in this paper, we find it by benefit the well-known brute-force search algorithm. In practical systems, θ_{opt} can be estimated from preamble data in each interval where CSI is estimated.

Figure (3) clearly shows the effect of CR on $\boldsymbol{Ix}_{11}^{R}$, and consequently the SINR. Using the brute-force search on interval $\theta \in [-\frac{\pi}{2}, \frac{\pi}{2}]$, SINR would maximize at a certain θ for each independent set of CSI realization. This rotation angle is called θ_{opt}. Further simulations and combination of PA and CR methods are prepared in the next section.

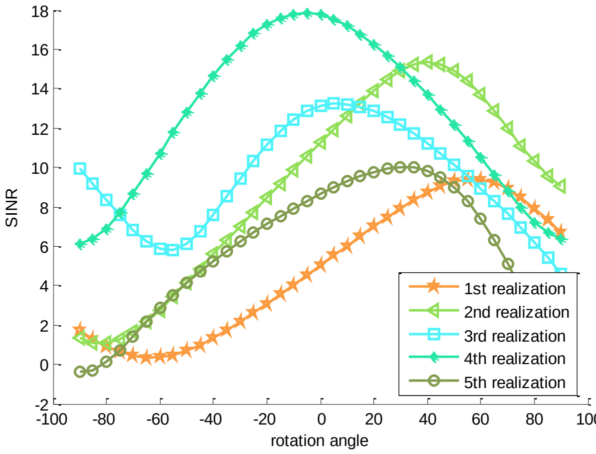

Fig. 3. SINR Variations compared to rotation angel for 5 independent set of CSI (ρ^2 =0.005 ,SNR=25 dB)

6. Computer simulations

In this section, we analyze the imperfect CSI effects on system performance and simulate the effect of PA on them. Computer simulations are provided in three subsections: system analysis without PA, with PA and with CR.

6.1. System analysis without PA

First, we analyze the imperfect CSI effects on BER of system and illustrate the performance degradation of system. For this purpose, consider constant rate BPSK modulation with varying SNR, P and variance of CSI error denoted as ρ^2.

Figure (4) shows the BER degradation versus SNR in some constant CSI errors ($\rho^2 = 0.001\,, 0.005\,, 0.01$).

In low SNR regime, the system performance is dominated by noise power and there is a slight difference in diagrams. But in high SNR regime, with increase of ρ^2, significant increase in BER is observed whereas, for example, achieving BER=10^{-4} for $\rho^2 = 0.001$ needs 4dB in SNR increment.

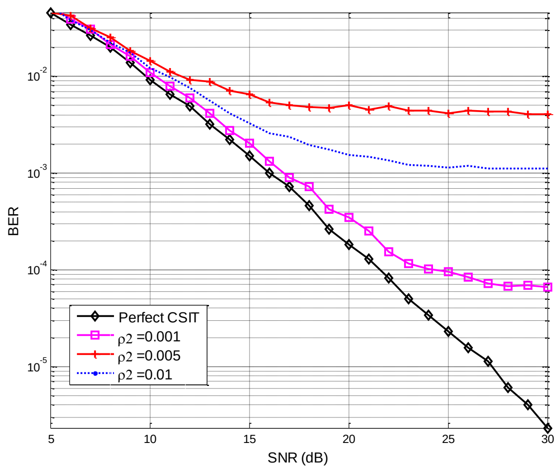

Fig. 4. system BER versus SNR for some constant CSI error variance (ρ^2)

Figure (5) shows BER degradation versus ρ^2 in some constant SNRs (SNR=10dB, 15dB, 20dB, and 25dB). This figure shows the linear increase of BER with increase of ρ^2.

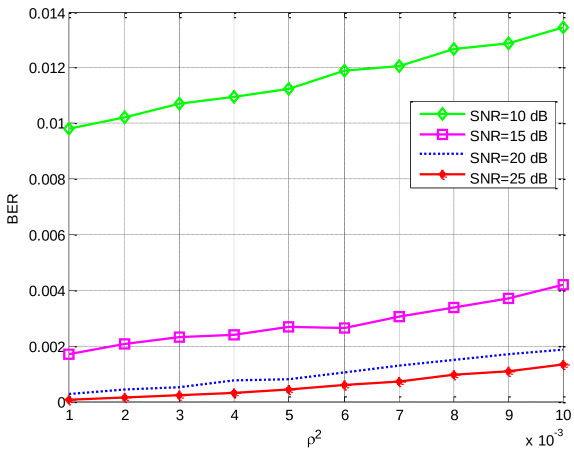

Fig. 5. system BER versus CSI error variance for some constant SNR

To illustrate the performance degradation caused by imperfect CSI, we define the following relation to represents the performance loss, compared to perfect CSI scenario:

$$Performance\ Loss = \frac{P\_CSI\_BER - Imp\_CSI\_BER}{P\_CSI\_BER} \qquad (34)$$

It is shown in figure (6) that the performance loss is linear and increase in SNR results in performance loss increment. However, the performance loss is negligible in low SNR for $\rho^2 = 0.001$.

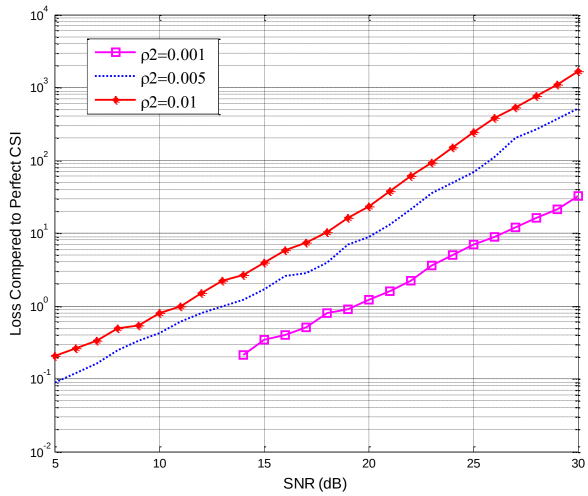

Fig. 6. BER performance loss versus SNR for some constant ρ^2

Since Alamouti coding is used for increasing diversity gain, the following definition is proposed to show the imperfect CSI effects on diversity gain:

$$G_d = -\lim_{SNR\to\infty} \frac{\log(Pe)}{\log(SNR)} \qquad (35)$$

Figure (7) shows that the diversity gain, in limitation case, tends to about 2 in perfect CSI, and tends to 1.4 in imperfect CSI with $\rho^2 = 0.001$ and even goes under 1 for $\rho^2 = 0.01$. This means that the diversity gain is not achieved in highly imperfect CSI channels and advantage of Alamouti coding is lost.

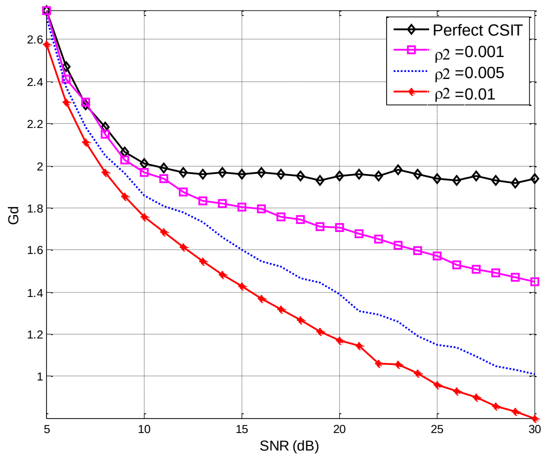

Fig. 7. diversity gain versus SNR for some constant ρ^2

As it is shown in (22), the SINR at high SNR regime is a proportional to $\frac{(1-\rho^2)}{\rho^2}$ and not related to transmit SNR. To illustrate this property, the received SINR is demonstrated in figure (8) with respect to ρ^2 for some values of transmit SNRs. It shows that the SINR for all transmit powers converge to a specific amount by increasing ρ^2. Thus, adding more transmit power cannot increase the SINR at the receiver. This can explain flatness of BER plot of figure (4) at high SNR regime.

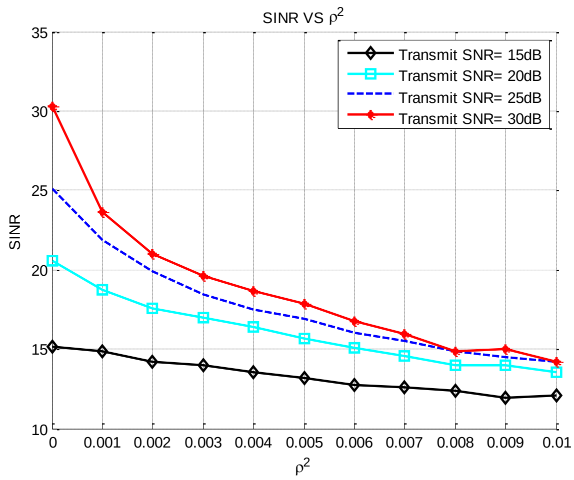

Fig. 8. Received SINR Versus ρ^2 for some constant transmit SNRs

6.2. System analysis with PA

The effect of PA improvement in imperfect CSI scenario is shown in figure (9). The brute-force search method is used on the interval [0, 1] to find the best (normalized) PA values for each ensemble of CSI where the system is simulated with founded PA ratio to calculate the BER. Simulation result shows 4dB SNR improvement to have BER=10^{-5} in perfect CSI and BER=10^{-4} in $\rho^2 = 0.001$ with the proposed PA algorithm.

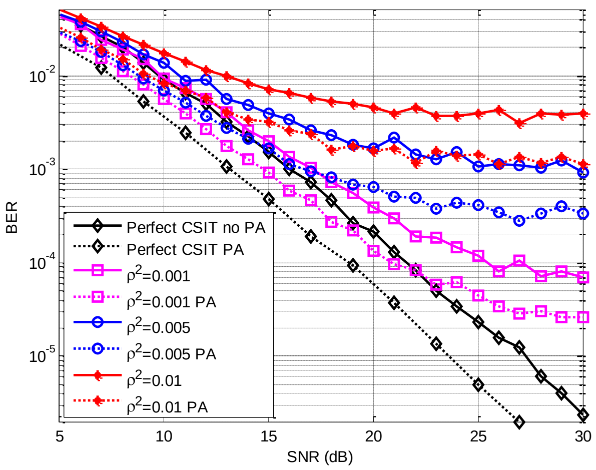

Fig. 9. BER performance with and without PA

To illustrate the effect of PA on system performance, SINR changes with respect to transmit SNR is proposed with and without PA for both perfect and imperfect CSI channel. The result which is presented in figure (10) shows desirable improvement in system SINR. This SINR improvement can reduce the BER of system which is shown in figure (9).

6.3. System analysis with CR

To calculate the effect of CR on system performance we assumed that CSI remains constant for 1000 samples and then new CSI with new error is desired. The algorithm uses brute-force search for $\theta \in [-\frac{\pi}{2}, \frac{\pi}{2}]$ interval and finds the best angle to minimize the $\boldsymbol{Ix}_{11}^{R}$ in equation (32). Then, 1000 samples using the founded θ_{opt} is transmitted at each constant CSI. Then, the algorithm repeats these steps until the number of error symbols raise to 1000. The BER simulation of this algorithm is compared with original imperfect CSI in figure (11) and it is shown a desirable improvement in BER performance. For example, simulation result shows 2.5dB SNR improvement to have BER=10^{-5} in perfect CSI and 3.5 dB SNR improvement to have BER=10^{-4} in $\rho^2 = 0.001$ with the proposed CR algorithm.

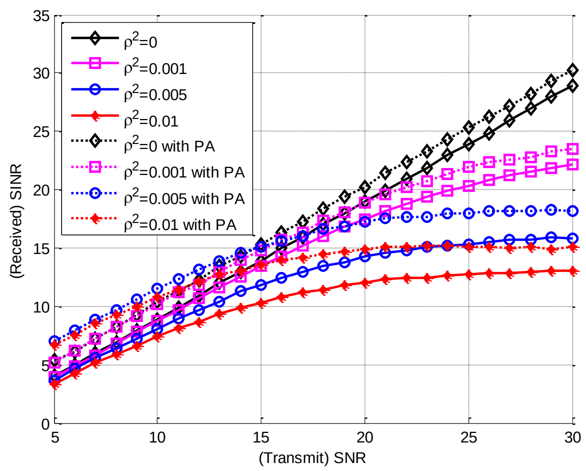

Fig. 10. SINR compared to transmit SNR with and without Power Allocation

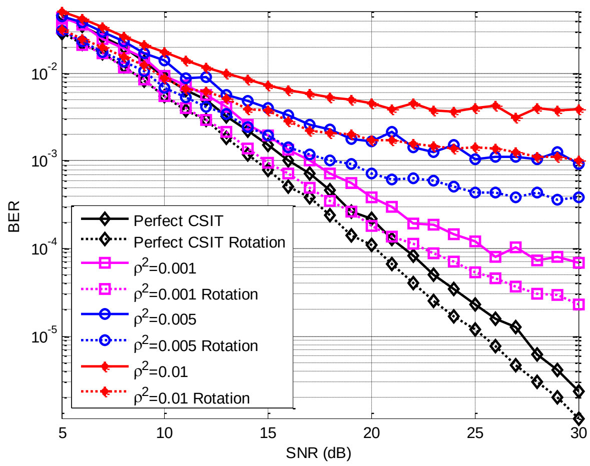

Fig. 11. BER performance with and without Constellation Rotation for deferent amount of CSI error (ρ^2)

6.4. Joint Power allocation and Constellation rotation performance Analysis

We can combine PA and CR methods and use them jointly to achieve better BER performance as Pa-CR method. To do this, first we find power allocation coefficients using equation (27). Then we found the best rotation angle for power allocated symbols using equation (33). Simulation result for joint PA-CR method shows effective improvement in BER performance. According to figure (12), the SNR improve 7dB to achieve BER=10^{-4} with $\rho^2 = 0.001$.

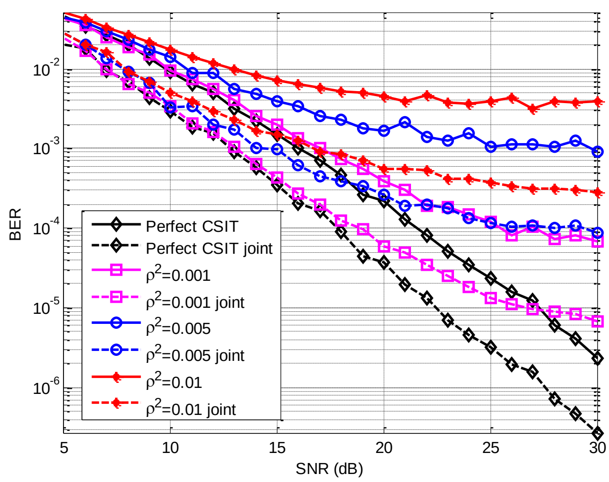

Fig. 12. BER performance with and without Joint PA-CR method for deferent amount of CSI error (ρ)

Figure (13) compare joint and single PA and CR methods with perfect and imperfect CSI for $\rho^2 = 0.001$. The results show that, joint PA-CR method can be used in Alamouti coded 2-user X-channel to achieve better BER performance at the lower SNR regime in imperfect CSI conditions.

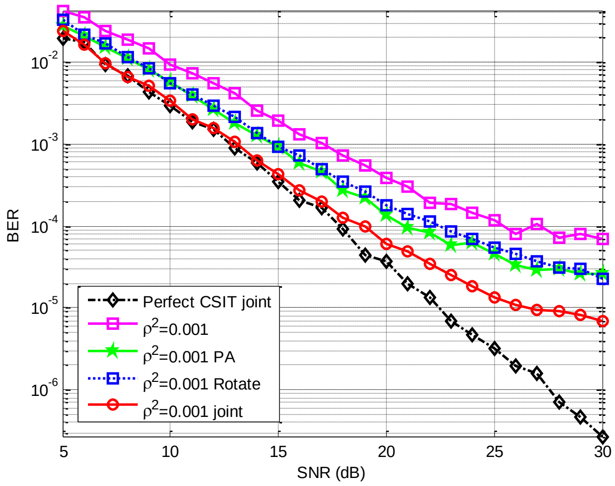

Fig. 13. BER performance comparison for PA method, CR method and joint PA-CR method for ρ^2=0.001

7. Conclusion

This paper analyzed the interference alignment and Alamouti coding under imperfect CSI condition and showed that the imperfect CSI effect can be separated from perfect CSI equations and separate into interference signal error and desired signal error. We showed that the BER of system varies linearly with respect to CSI error variance. Moreover, CSI error degrades diversity gain which achieved by Alamouti coding and if CSI error exceeds $\rho^2 = 0.01$, the diversity gain goes under 1. Also, the result show that received SINR is bounded at high SNR regime with imperfect CSI and it's bound is proportional to $\frac{(1-\rho^2)}{\rho^2}$. This means that we cannot achieve arbitrary low BER by only increasing the transmit SNR. Then, we proposed Power Allocation algorithm, Constellation Rotation algorithm and combined them as Joint PA-CR algorithm to improve the performance of system in imperfect scenario. The results show that the proposed Joint PA-CR can improve the BER floor of system and also improve the required SNR to have the same BER about 7dB to have BER=10^{-4} in $\rho^2 = 0.001$ and BER=10^{-3} in $\rho^2 = 0.005$. Computer simulation confirm the attained analysis. The obtained results can help the future researches to improve the system performance under imperfect CSI or decrease the effect of each term of error.

8. REFERENCES

[1] M. Maddah-Ali, A. Motahari, and A. Khandani, “Communication over X channel: Signalling and multiplexing gain”, Technical Report, University of Waterloo, 2006.

[2] V. Cadambe and S. Jafar, “Interference alignment and the degrees of freedom of the K user interference channel", IEEE Transaction on Information Theory, vol. 54, no 8, pp. 3425-3441, 2008.

[3] K. Gomadam, V.R. Cadambe, S. A. Jafar, “Approaching the capacity of wireless networks through distributed Interference alignment”, IEEE Global Telecommunications Conference (GLOBECOM), New Orleans, USA, Dec. 2008, pp. 1-6.

[4] Viveck R. Cadambe, Syed A. Jafar, “Interference alignment and the degrees of freedom of wireless X networks", IEEE Transactions on Information Theory, vol. 55, no.9, pp. 3893-3908, 2009.

[5] C. Suh, D. Tse, “Interference alignment for cellular networks”, 46th Annual Alerton Conference on Communications, Control and Computing, Monticello, USA, Sep 2006, pp.1037-1044.

[6] M. Maddah-Ali, A. Motahari, and A. Khandani, “Communication over MIMO X channels: Interference alignment, decomposition, and performance analysis", IEEE Transaction on Information Theory, vol. 54, n0. 8, pp. 3457-3470, 2008.

[7] S.A. Jafar, “Exploiting channel correlations Simple interference alignment schemes with no CSIT,” IEEE Global Telecommunications Conference, Miami, USA, Dec. 2010, pp.1-5.

[8] Liangbin Li, H. Jafarkhani, S.A. Jafar, “ When alamouti codes meet interference alignment: Transmission schemes for two-user X channel”, Proceedings of IEEE International Symposium on Information Theory, Petersburg, Russia, Jul 31-Aug 5, 2011, pp. 2577-2581.

[9] B. Xie,Yang Li, H. Minn, A. Nosratinia,” Adaptive interference alignment with CSI uncertainty”, IEEE Transaction on Communications, vol. 61, no. 2, pp. 792-801, 2013.

[10] Nosrat-Makouei, B. , Andrews, J.G. , Heath, R.W.“MIMO Interference alignment over correlated channels with imperfect CSI”, IEEE Transaction on Signal Processing, vol. 59, no. 6, pp. 2783-2794, 2011.

[11] Tresch R.,Guillaud M., “Cellular interference alignment with imperfect channel knowledge”, IEEE International Conference on Communication Workshops (ICC), Dresden, Germany, June 2009, pp. 1-5.

[12] T. G. Gou, C. W. Wang, S. A. Jafar, “Aiming perfectly in the dark-blind interference alignment through staggered antenna switching,” IEEE Transaction on Signal Processing, vol. 59, no. 6, pp. 2734–2744, 2011.

[13] S.A Jafar, “Blind interference alignment”, IEEE Journal of Selected Topics in Signal Procesing, vol. 6, no. 3, pp. 216-227, 2012.

[14]. C. Wang, H. C. Papadopoulos, S. A. Ramprashad, G. Caire, “Design and operation of blind interference alignment in cellular and cluster-based systems”, Information Theory and Applications Workshop (ITA), Jolla, USA, Feb 2011, pp. 1-10

[15] X. Chen and C. Yuen, "On Interference Alignment With Imperfect CSI: Characterizations of Outage Probability, Ergodic Rate and SER," in *IEEE* Transactions on Vehicular Technology, vol. 65, no. 1, pp. 47-58, 2016.

[16] W. Liu, X. Li, D. Wang, Q. Cheng and Y. Wang, "Imperfect CSI impact on sum-rate performance of IA: A comprehensive analysis," in IEEE 28th Annual International Symposium on Personal, Indoor, and Mobile Radio Communications (PIMRC), Montreal, Canada, 2017, pp. 1-7.

[17] D. S. Jin, J. H. Kim and J. S. No, "Combining interference alignment and Alamouti codes for quasi-

static MIMO X channel," 18th Asia-Pacific Conference on Communications (APCC), Jeju, South Korea, 2012, pp. 939-940.

[18] Z. Mingjie, L. Bihong , "Performance Analysis of Alamouti Scheme With Imperfect Multiple Transmit Antennas Selection in Rayleigh Fading Channel", 7th International Symposium on Antennas, Propagation & EM Theory, Guilin, China, 2006, pp. 1-4.

[19] R. F. Guiazon, K. K. Wong, M. Fitch, "Coverage probability of cellular networks using interference alignment under imperfect CSI", Digital Communications and Networks, vol. 2, no. 4, pp. 162-166,2016.

[20] J. Kim, D. Jin, X. Jin, J. No and D. Shin, "Interference alignment-and-cancellation scheme based on Alamouti code for the three-user MIMO interference channel", IET Communication, vol. 9, no. 10, pp. 1278-1288, 2015.

[21] D. Song, W. Shin and J. Lee, "Interference Alignment Based on Alamouti Code for M ×2 X-Channels with Multiple Antennas," IEEE 83rd Vehicular Technology Conference (VTC), Nanjing, China, 2016, pp. 1-5.

[22] X. Tian, D. Yang, H. Zhang and W. Jia, "Improved Interference Cancellation Scheme for X Channels with Four Antennas", Journal of Computer and Communications, vol. 5, no. 6, pp. 57-64, 2017.

[23] Z. Kong, S. Peng, Y. Zhang, L. Zhong, "EIV-Based Interference Alignment Scheme with CSI Uncertainties", Mathematical Problems in Engineering, vol. 2015, pp. 1-11, 2015.

[24] H. Khaleghi Bizaki, A. Falahati, "Tomlinson Harashima Precoder with Imperfect Channel State Information ", IET Communication Journal, vol. 2, no. 1, pp. 151 – 158, 2008.

[25] G. Taricco and E. Viterbo, "Performance of component interleaved signal sets for fading channels," Electronics Letters, vol. 32, no. 13, pp. 1170-1172, 1996.

[26] S. B. Slimane, "An improved PSK scheme for fading channels," IEEE Transaction on Vehicular Technology, vol. 47, no. 2, pp. 703-710, 1998.

[27] J. Boutros and E. Viterbo, "Signal space diversity: a power and bandwidth-efficient technique for the Rayleigh fading channel," IEEE Transaction on Information Theory, vol. 44, no. 4, pp. 1453-1467, 1998.

[28] T. Kurt and H. Delie, "Transmitter diversity for robustness to channel estimation errors", IEEE Electronics Letters, vol. 41, no. 5, pp. 263-265, 2005.

[29] T. Jung and K. Cheun, "Design of concatenated space-time block codes using signal space diversity and the Alamouti scheme", IEEE Communication Letters, vol. 7, no. 7, pp. 329-331, 2003.

[30] V. Tarokh, A. Naguib, N. Seshadri and A. R. Calderbank, "Space-time codes for high data rate wireless communication: performance criteria in the presence of channel estimation errors, mobility, and multiple paths", IEEE Transactions on Communications, vol. 47, no. 2, pp. 199-207, 1999.

[31] S. Jeon, J. Lee, I. Kyung, M. Kim, "Component interleaved Alamouti coding with rotated constellations for signal space diversity", IEEE Intternational Symposium on Broadband Multimedia Systems and Broadcasting (BMSB), Shanghai, China, 2010, pp. 1-6.

[32] H. K. Bizaki, M. K. Hojaghan, S. M. Razavizadeh, "Power optimization of tilted tomlinson-harashima precoder in MIMO channels with imperfect channel state information", Journal of Optimization (Hindawi), 2013.

[33] M. Nezam abadi and A. Falahati, "Opportunistic interference alignment in cognitive radio networks with transmitting space time code for secondary users", Journal of Electrical engineering, vol. 76, no. 2, pp. 333-341, 2016.

[34] E. Dashtian, M. Okhovat, H. Arezomand, "MIMO Channel Estimation by QR Decomposition and LMS Adaptive Filter", Journal of Electrical engineering, vol. 48, no. 2, pp. 609-616, 2018.